Article

A *cis*-Acting Element in Retroviral Genomic RNA Links Gag-Pol Ribosomal Frameshifting to Selective Viral RNA Encapsidation

Mastooreh Chamanian,[1] Katarzyna J. Purzycka,[2] Paul T. Wille,[3] Janice S. Ha,[3] David McDonald,[1] Yong Gao,[1,3] Stuart F.J. Le Grice,[2] and Eric J. Arts[1,3,*]
[1]Department of Molecular Biology and Microbiology, Case Western Reserve University, Cleveland, OH 44106, USA
[2]RT Biochemistry Section, HIV Drug Resistance Program, National Cancer Institute, Fredrick, MD 21702, USA
[3]Department of Medicine, Case Western Reserve University, Cleveland, OH 44106, USA
*Correspondence: eja3@case.edu
http://dx.doi.org/10.1016/j.chom.2013.01.007

SUMMARY

During retroviral RNA encapsidation, two full-length genomic (g) RNAs are selectively incorporated into assembling virions. Packaging involves a *cis*-acting packaging element (Ψ) within the 5′ untranslated region of unspliced HIV-1 RNA genome. However, the mechanism(s) that selects and limits gRNAs for packaging remains uncertain. Using a dual complementation system involving bipartite HIV-1 gRNA, we observed that gRNA packaging is additionally dependent on a *cis*-acting RNA element, the genomic RNA packaging enhancer (GRPE), found within the *gag* p1-p6 domain and overlapping the Gag-Pol ribosomal frameshift signal. Deleting or disrupting the two conserved GRPE stem loops diminished gRNA packaging and infectivity >50-fold, while deleting *gag* sequences between Ψ and GRPE had no effect. Downregulating the translation termination factor eRF1 produces defective virus particles containing 20 times more gRNA. Thus, only the HIV-1 RNAs employed for Gag-Pol translation may be specifically selected for encapsidation, possibly explaining the limitation of two gRNAs per virion.

INTRODUCTION

Retroviral RNA encapsidation is a highly ordered process by which two full-length genomic (g) RNAs are incorporated into assembling virions. Although a single gRNA template can support retroviral reverse transcription and proviral DNA synthesis (Hu and Temin, 1990), recombination and reassortment of polymorphisms is a hallmark feature of the retrovirus and dependent on a diploid genome. Prior to packaging, intergenomic annealing initiates formation of loose noncovalent dimers of unspliced HIV-1 RNA, which is then selected for encapsidation over the excess host cellular and viral spliced HIV-1 RNAs (~99% of the total cellular RNA). This selectivity is due to the recognition of a *cis*-acting packaging element within the 5′ untranslated region (5′UTR) by the nucleocapsid (NC)

domain of the Gag polyprotein via two zinc fingers (Berkowitz et al., 1996; Rein, 1994; D'Souza and Summers, 2005). Confocal microscopy studies suggest that the capture of gRNA by Gag occurs in a perinuclear/centrosomal site. A single interaction with gRNA may nucleate Gag multimerization during assembly (Burniston et al., 1999; Kutluay and Bieniasz, 2010), or multiple Gag proteins may preassemble into oligomeric arrays in the cytoplasm prior to gRNA binding (Swanson and Malim, 2006). It remains unclear why only one gRNA dimer is bound to one of 2,000 Gag dimers forming new virus particles (Davis and Rueckert, 1972) rather than one gRNA dimer per Gag protein.

Secondary and tertiary structures of retroviral gRNAs in the 5′UTR as well as proximal coding regions are involved in gRNA dimerization, packaging, and translation (Lu et al., 2011; Damgaard et al., 2004; Abbink and Berkhout, 2003). In HIV-1, the canonical packaging signal (also referred to as psi or Ψ) contains four stem loops (SL1–SL4) located downstream of the primer binding site (PBS) and extending into the 5′ terminus of *gag* coding sequences (Lever et al., 1989; Aldovini and Young, 1990). In particular, SL1 contains the dimerization initiation site (DIS) which forms the kissing loop for gRNA dimerization (Johnson and Telesnitsky, 2010; Skripkin et al., 1994). Both SL2 (containing the splice donor site) and SL3 have high affinity for NC (Amarasinghe et al., 2000), but only SL3 is recognized as the core packaging element containing the highly conserved GGAG NC-binding sequence (De Guzman et al., 1998). In complex retroviruses such as HIV-1, gRNA packaging and dimerization signals map to multiple sequences in both LTRs and the 5′ end of *gag*, including the *trans*-activating-responsive (TAR) stem loop and PBS (Russell et al., 2003; McBride and Panganiban, 1996; Clavel and Orenstein, 1990). Despite attempts to define the complete HIV-1 gRNA packaging signal, the relative role of each sequence within HIV-1 genome has remained debatable.

Understanding lentivirus gRNA packaging is important to aspects of HIV-1 replication/pathogenesis, development of drug targets, and enhancement of lentiviral gene delivery or vaccine efficacy. In this study, the HIV-1 g/mRNA was subdivided into two subgenomic (sg) RNA species where both contain at least Ψ required for encapsidation. Only one sgRNA acts as a template for reverse transcription such that mutations/deletions in this RNA can be evaluated for effects on
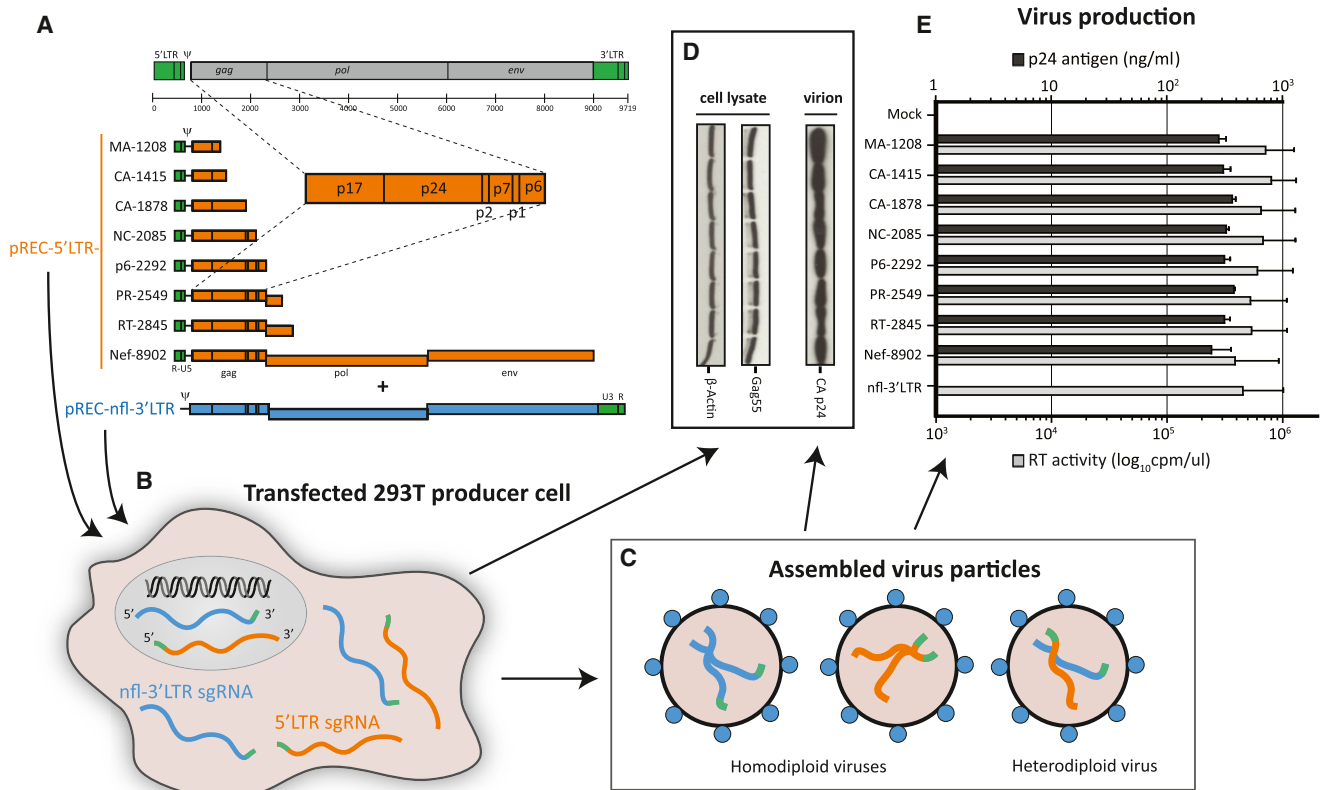
Figure 1. Complementation System Used for Packaging Studies and Infectious Virus Production

(A) Series of pREC-5′LTR HIV-1 vectors were constructed to express incremental lengths of HIV-1 subgenomic (sg) RNA. The plasmid depicted in orange harbors the 5′LTR followed by various HIV-1 coding sequence. The pREC-nfl-3′LTR (near full length or nfl) HIV-1 vector (in blue) lacks the 5′LTR and is used to cotransfect 293T cells and complement the pREC-5′LTR. (B) Both vectors express 5′-capped, 3′ poly(A) HIV-1 mRNA species for the full complement HIV-1 proteins in the cells and produce virus particles indistinguishable from those derived for transfection with full-length proviral DNA constructs (e.g., pNL4-3) (Dudley et al., 2009). 293T transfectants produce three virus types (C) containing either two 5′LTR sgRNAs (x), two nfl-3′LTR sgRNAs (y), or one of each (heterodiploid or xy). As described in Figure S2, the 5′LTR and nfl-3′LTR sgRNAs in the heterodiploid virus can complement each other during reverse transcription to generate a WT, full-length proviral DNA where the coding sequence is only derived from the nfl-3′LTR. At 48 hr posttransfection, virus produced from 293T cells transfected with pREC-nfl-3′LTR and pREC-5′LTR was monitored by western blots using anti-p24 and anti-β actin (as control for cellular protein expression) in cell lysates or in virus-containing supernatants (D). (E) Virus production was also measured in supernatants by measuring RT activity using a radiolabelled assay or by quantifying CA p24 using an antigen capture assay. Data are presented as mean ± SEM. See also Figure S2.

packaging independent of the underlying coding sequence. Using this system, efficient gRNA encapsidation maps to two general regions: Ψ in the 5′UTR and a genomic RNA packaging enhancer (or GRPE) element which overlaps with the ribosomal frameshift site (~1,200 nt downstream from Ψ). A programmed −1 nt ribosome frameshifting occurs at the Gag-Pol ribosomal frameshift signal (RFS) of unspliced HIV-1 mRNA during Gag translation, leading to production of the Gag-Pol precursor protein (Jacks et al., 1988; Wilson et al., 1988). Recently, the ribosomal stimulatory hairpin structure in HIV-1 RFS (Dulude et al., 2002) or P3 stem loop (P3SL) as well as stable stem loop (P2 stem loop or P2SL) has been defined by SHAPE RNA structure analyses (Watts et al., 2009). In most retroviruses (aside from lentiviruses), a similar region at the 3′ terminus of *gag* forms a pseudoknot that regulates ribosomal pausing (Jacks et al., 1988). Our findings now suggest a possible coregulation of HIV-1 Gag-Pol translation and gRNA packaging during virus production and assembly.

RESULTS

An HIV-1 Replication System Involving Bipartite HIV-1 gRNA Where Only One Contributes to the Coding Sequence

Research on gRNA packaging has focused primarily on signature RNA sequences or secondary structures in the 5′UTR (Lever et al., 1989; Clavel and Orenstein, 1990; Lu et al., 2011; McBride and Panganiban, 1996). Mapping potential RNA packaging elements within the HIV-1 coding region is more challenging, considering confirmatory mutagenesis requires synonymous substitutions to maintain the proteome while altering RNA structure/sequence. For these reasons, we cotransfected the 293T producer cells with the two plasmids expressing two sgRNAs (Dudley et al., 2009) (Figures 1A and 1B). Briefly, the minimal CMV promoter in pREC-5′LTR-nfl expresses a sgRNA starting from R (nt 456; HXB2 genome numbering) and ending prior to U3 (Nef-8902nt) with the BGH poly(A) (Figure 1A, last plasmid

and RNA depicted in orange), whereas the complementing vector pREC-nfl-3′LTR expresses sgRNA starting at PBS and ending with the U3-R, and HIV-1 poly(A) (termed 3′LTR for this article) (Figures 1A and 1B, plasmid and RNA depicted in blue). HIV-1 mRNA expression from the CMV promoter may be slightly reduced from that observed from the HIV-1 LTR promoter, but the 5′LTR-nfl still contains the TAR sequence and is stimulated by Tat. In contrast, the nfl-3′LTR lacks the TAR involved in abortive transcription.

Both sgRNAs from pREC-5′LTR-nfl and pREC-nfl-3′LTR are derived from the NL4-3 clone, harbor Ψ, and can act as mRNA templates for translation of HIV-1 structural proteins in transfected cells. As expected, the truncated 5′LTR sgRNAs did not produce truncated Gag precursor proteins in the cells (see Figure S1 online). If both the 5′LTR-nfl and nfl-3′LTR sgRNAs are encapsidated at equal efficiencies, 50% of the virus particles will be heterodiploid for both sgRNAs (based on Hardy-Weinberg equilibrium X^2+Y^2+2XY) (Figure 1C) (Dudley et al., 2009). Due to lack of the U3-R or R-U5 sequences, homodiploid viruses with two copies of 5′LTR-nfl or nfl-3′LTR sgRNAs are unable to complete reverse transcription following de novo entry into a host cell (depicted in Figures S2A–S2C). In contrast, infection with the heterodiploid virus leads to completion of reverse transcription, reconstitution of a full-length wild-type (WT) genome, and proviral DNA integration (Figures S2A and S2D).

The entire HIV-1 proteome originates from the nfl-3′LTR sgRNA following de novo infection with heterodiploid virus, whereas the 5′LTR-nfl sgRNA only serves a template for tRNA^{Lys,3} binding and synthesis of (−) strand strong-stop DNA (Figure S2D). As described below, we have introduced some large deletions, multiple point mutations, and insertions into the coding region of 5′LTR-nfl sgRNA without impacting on RNA packaging or infectivity, whereas other mutations have significant effects. Although the elongating HIV-1 DNA during reverse transcription could jump between the nfl-3′LTR and 5′LTR-nfl sgRNA templates, our high level of infectivity with or without deletions suggests that these recombination events occur at a relatively low frequency (estimated at 10%) (Dudley et al., 2009).

Locating *cis*-Acting RNA Elements in the HIV-1 Coding Sequence Necessary for gRNA Encapsidation

When pREC-nfl-3′LTR construct was cotransfected with the pCMV_cplt construct (expressing a short sgRNA containing R-U5-PBS-MA) in a previous study, the resulting virus was minimally infectious compared to WT NL4-3 virus (<0.01% infectivity) (Dudley et al., 2009). Although the absolute level of viral RNA was similar to that in WT HIV-1 particles, we determined that this reduced infectivity was attributable to poor packaging of this short 5′LTR sgRNA compared to the nfl-3′LTR sgRNA, despite the fact that both sgRNAs harbored Ψ. As described below, we noticed that WT infectivity was rescued by extending the short 5′LTR sgRNA to a near full-length HIV-1 RNA genome. Based on these observations, we surmised that a previously unrecognized site within the coding sequence of the HIV-1 genome was necessary for efficient RNA packaging.

To crudely map the coding region that contributes to gRNA packaging, we deleted incremental amount of segments from

the 3′ terminus of proviral genome within the pREC-5′LTR-nfl vector to produce sgRNA (upon transfection) starting with the R-U5 but ending at Nef$_{8902}$, RT$_{2845}$, PR$_{2549}$, p6$_{2292}$, NC$_{2085}$, CA$_{1878}$, CA$_{1415}$, or MA$_{1208}$ (Figure 1A, see Table S1 for HXB2 genomic RNA numbering). For all cotransfections, Gag protein expression in cells and capsid (CA) in viruses were monitored by western blot and ELISA (Figures 1D and 1E), and RT activity was measured in the cell-free supernatant (Marozsan et al., 2004) (Figure 1E). Transfections with pREC-nfl-3′LTR alone or cotransfections of the pREC-nfl-3′LTR with the various pREC-5′LTR vectors produced similar amounts of virus based on RT activity (Figure 1E).

A stock of WT NL4-3 HIV-1 and virus derived from 293T transfections were serially diluted to measure RT activity and to infect U87-CD4-CXCR4 cells (Figures 2A, 2C, and 2D). We have previously shown that RT activity of a WT HIV-1 stock is a strong correlate of its infectious titer (Marozsan et al., 2004). Based on the linear regression equation from RT activity versus infectious titer of an NL4-3 virus stock (Figure 2B), we estimated that each virus from cotransfections would have a similar infectious titer as shown in Figure 2E. However, the actual serial dilution/infection in U87-CD4-CXCR4 revealed a significant drop in infectious titer with viruses that should have contained the shorter 5′LTR (NC$_{2085}$, CA$_{1878}$, CA$_{1415}$, or MA$_{1208}$) sgRNA compared to the longer 5′LTR (Nef$_{8902}$, RT$_{2845}$, PR$_{2549}$, and p6$_{2292}$) sgRNA (Figure 2F). Based on this deletion mapping, it appears that a 207 nt sequence within the p1–p6 coding region (between NC$_{2085}$ and p6$_{2292}$ in the 5′LTR sgRNA) was responsible for a >350-fold increase in infectious titers. Even inclusion of another 6,600 nt of sequential HIV-1 genome sequence on the 5′LTR sgRNA (e.g., Nef 8902; Figure 1A) failed to further increase infectivity (Figure 2F). However, shortening the 5′LTR sgRNA from NC$_{2085}$ to CA$_{1878}$ (Figure 1A) resulted in an additional 10-fold loss of infectivity, i.e., >3,000-fold less infectious than the heterodiploid virus potentially containing the 5′LTR-p6$_{2292}$ and nfl-3′LTR sgRNAs (Figure 2F).

The GRPE RNA Element Is Necessary for Infectivity via Effects on gRNA Packaging

Since reduced infectivity with the 5′LTR sgRNA truncations was not due to disruption of virus particle formation or release, we suspected that gRNA encapsidation might have been compromised. First, we confirmed that 5′LTR and 3′LTR sgRNAs were efficiently expressed in the cells by showing that cellular-associated viral sgRNA levels, normalized to 18S ribosomal RNA levels, were not affected by the length of the 5′LTR sgRNA (Figure S3B). Encapsidation of both sgRNAs can be measured using quantitative reverse transcriptase PCR (qRT-PCR) with 5′LTR- and 3′LTR-specific primers and probes (Figure 3A). To ensure that viral RNAs were transported from the nucleus, cells were partitioned into cytoplasmic and nuclear fractions. The presence of only spliced β-actin mRNA in the cytoplasmic fraction confirmed efficient separation from the nuclear fraction (Figure S3A). There were, however, abundant and similar levels of the unspliced 5′LTR sgRNAs and nfl-3′LTR sgRNA in the cell cytoplasm (Figure S3C). HIV-1 Rev binding to the Rev-responsive element (RRE) in the *env* gene rescues unspliced and partially spliced HIV-1 RNA transcripts from the nucleus for transport to the cytoplasm. It is unlikely that Rev would increase transport of the
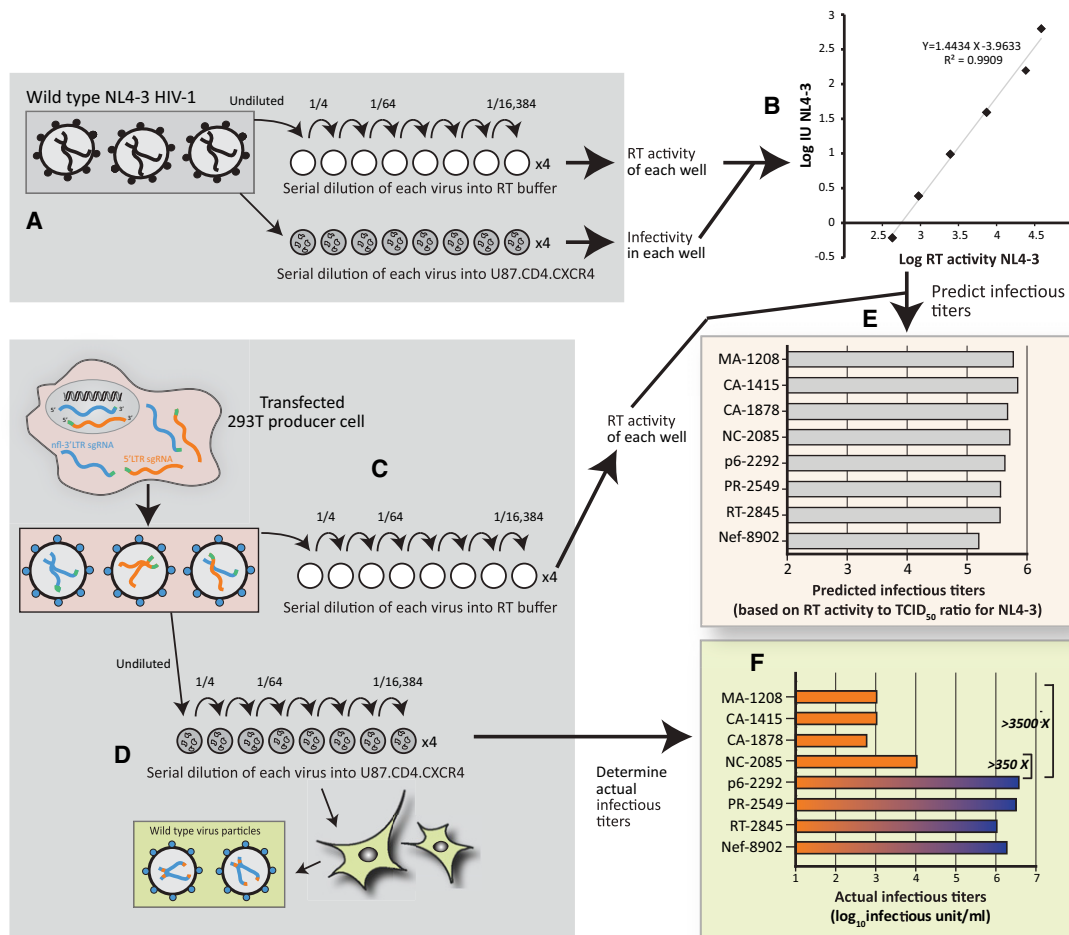
Figure 2. Comparing the Expected and Actual Infectious Titers of Virus Derived from Cotransfected 293T Cells

(A) Wild-type NL4-3 HIV-1 was serially diluted (1:4) and used to measure RT activity and to infect U87.CD4.CXCR4. (B) RT activity was plotted against the level of virus production for each dilution to determine a linear regression formula and to obtain as a surrogate of infectious titer (Marozsan et al., 2004). Virus produced from the cotransfected 293T cells was diluted to measure RT activity (C) or to infect U87.CD4.CXCR4 cells (D). (E) provides the estimated infectious titers based on analyses from (B) and (C). The actual $TCID_{50}$ values (F) were derived from the serial dilution/infections of the U87.CD4.CXCR4 cells (D) using the standard limiting protocol (Marozsan et al., 2004). The values are plotted at log_{10} infectious units/ml. See also Figure S1.

5′LTR sgRNA transcripts, because all but 5′LTR-Nef$_{8902}$ sgRNA lack the RRE as well as all known splice acceptor sites. In monotransfections with the pREC-5′LTR vectors and in the absence of Rev (provide by the pREC-nfl-3′LTR), we still detected high levels of unspliced HIV-1 RNA in cytoplasmic fractions (data not shown).

The level of sgRNAs in virus was measured to determine packaging efficiency of the different 5′LTR sgRNAs (Figure 3B) relative to nfl-3′LTR sgRNA (Figure 3C). A dramatic shift was observed in 5′LTR sgRNA packaging when this RNA was extended into the p6 region of the *gag* coding sequence (27-fold increase in packaging of 5′LTR-p6$_{2292}$ sgRNA packaging over 5′LTR-NC$_{2085}$ sgRNA, respectively [Figure 3B]). However, extension of the HIV-1 RNA genome beyond nt 2,292 (to near full length) did not augment gRNA packaging. Relative encapsidation of the different 5′LTR sgRNA directly correlated with the level of virus infectivity (compare Figure 3B and Figure 2F). Interestingly, the levels of efficient nfl-3′LTR

sgRNAs in virus particles remained relatively constant despite reduced 5′LTR sgRNA packaging (Figure 3C).

As a control, the AUG *gag* start codon was deleted in some of the 5′LTR sgRNAs (Figures 3D and 3E) such that any recombination would result in formation of dead virus, and yet we did not observe an effect on RNA packaging or infectivity, suggesting that this low-frequency recombination was not affecting the primary results with our system.

Reduced HIV-1 Genomic RNA Encapsidation with GRPE Deletion

Based on our truncation analyses, we mapped a putative packaging determinant, designated the GRPE, to a 200–400 nt RNA sequence at the 3′ end of *gag*. To confirm the role of the putative GRPE in genome encapsidation, two fragments containing GRPE and surrounding sequences were deleted from pREC-5′LTR-RT$_{2845}$ plasmid (Figure 4A). Encapsidation of the 5′LTR-RT$_{2845}$ sgRNA with these GRPE deletions was
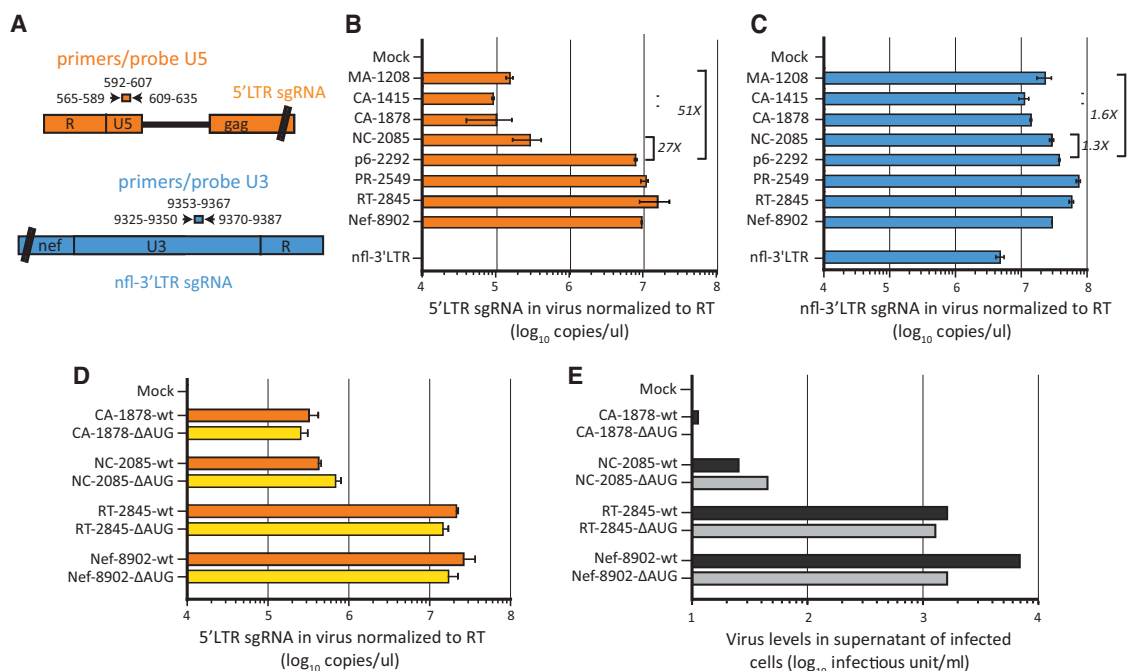
Figure 3. Relative Packaging of the HIV-1 Subgenomic RNA in Virus Derived from Cotransfected Cells

pREC-5′LTR plasmids were used to transfect 293T cells along with pREC-nfl-3′LTR. (A) Schematic representation of primers and probes used to specifically PCR amplify and quantify the 5′LTR sgRNA (orange) and nfl-3′LTR sgRNA (blue) following cDNA synthesis (see Table S2 for primer details). Viral RNA was extracted from cell-free supernatants of transfected cells. Copy numbers of 5′LTR sgRNA (B) and nfl-3′LTR sgRNA (C) were determined by qRT-PCR, compared to qRT-PCR amplification of in vitro-transcribed HIV-1 RNA of known copy number (10^4 to 10^{10} copies), and presented as relative to the viral RT activity. Figure S3 presents the cytoplasmic and cellular levels of sgRNAs prior to packaging. (D) RNA packaging efficiency was not influenced by deletion of a Gag AUG start codon in the 5′LTR sgRNAs. Gag AUG initiation codon was deleted in the pREC-5′LTR-CA $_{1878}$, NC$_{2085}$, RT$_{2845}$, and Nef$_{8902}$. Viral RNA was extracted from cell-free supernatants of transfected cells. Copy numbers of WT and ΔAUG 5′LTR sgRNAs were determined by qRT-PCR and normalized to the viral RT activity. (E) Virus infectivity was measured by first normalizing for RT activity, serially diluted as described in Figure 2D, and then added to U87.CD4.CXCR4 cells, i.e., a standard TCID$_{50}$ assay. The level of infectious virus is presented as $\log_{10}$ infectious units/ml. Data in (B)–(D) are presented as mean ± SEM. See also Figure S3.

reduced >14-fold (Figure 4B), while the nfl-3′LTR sgRNAs were encapsidated at similar level (Figure S4A). The reduced 5′LTR sgRNA in the absence of the GRPE corresponded to a >80-fold decrease in virus infectivity (Figure 4C). Based on 3′ truncation and deletion analyses, we could map the GRPE to ~200 nt between 1,956 nt and 2,188nt (RNA# 1,500 nt–1,732 nt) in the HIV-1 genome which also encompasses RFS. Again, the 5′LTR sgRNA neither contributes appreciably to HIV-1 protein production nor impacts virus particle formation and release, but must be copackaged with the nfl-3′LTR sgRNA for subsequent virus propagation.

Investigating the impact of the GRPE deletion in the full-length HIV-1 construct is problematic due to simultaneous deletion of the Gag open reading frame, which prevents virus production. To compensate, Gag and Gag-Pol proteins were provided in *trans* from pCMVΔR8.91 helper plasmid cotransfected with WT and ΔGRPE pNL4-3 HIV-1. Due to the 3′-Gag/GRPE deletion, the virus derived from these 293T transfections was limited to a single round of infection and could not be propagated as with the bipartite genome system. Virus from transfections was harvested, equalized for RT activity, and then lysed to measure gRNA content. Virus particles derived from the WT versus pNL4-3ΔGRPE contained 7-fold more gRNA (p < 0.001) (Figure 4D).

Positional Dependence of GRPE for gRNA Encapsidation

To further map the GRPE, investigate its positional dependence, and determine its minimal structure, sequences between the GRPE and Ψ in the 5′LTR sgRNAs (ending at nucleotides 2,292, 2,270, and 2,183 in p6) were deleted by yeast recombination/gap repair to generate 5′LTR-p6Δ868, Δ716, Δ706, and Δ996 sgRNAs (Figure 4E). The resulting RNAs lack most of the *gag* MA/CA/NC coding sequence but retain different p7/p1/p6 coding regions housing the GRPE. Packaging efficiencies and infectivities were investigated with the bipartite genome/complementing system. To better understand the behavior of these gRNA constructs, domains within and around the GRPE were structurally characterized using SHAPE (Watts et al., 2009), which involves exposing RNAs to a reactive anhydride (1M7) that selectively acylates ribose 2′-OH moieties within flexible (i.e., usually single-stranded) nucleotides. Sites of chemical modification are subsequently detected as stops during reverse transcription, and the products are fractionated by electrophoresis. RNA secondary structures were predicted by introducing constraints derived from chemical probing data into RNA structure (Mathews et al., 2004). Full-length in vitro-transcribed 5′LTR sgRNA constructs were used for structural probing, although acylation profiles presented here are restricted to regions involved in RNA packaging (Figure 4H).
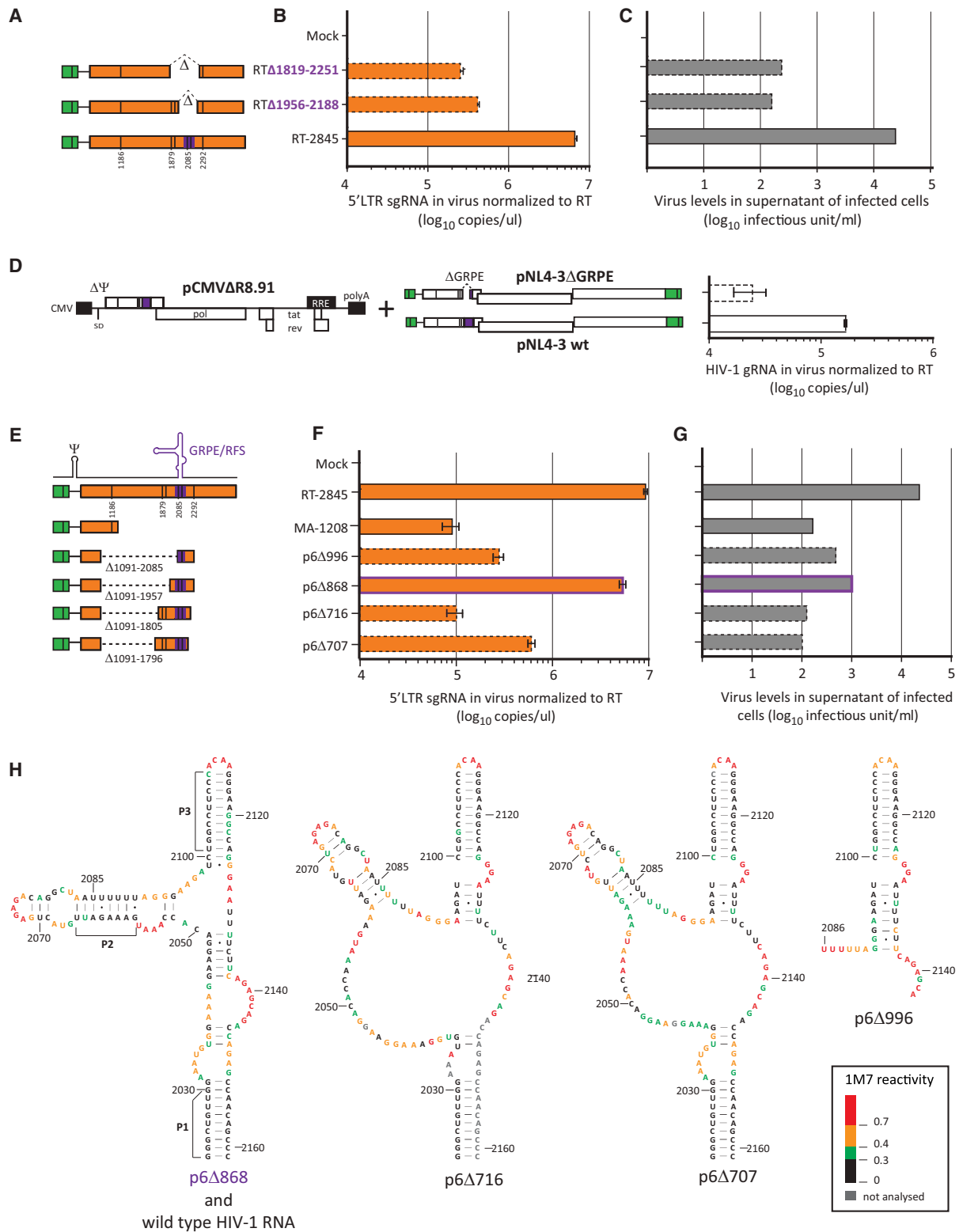
Figure 4. Effect of Deleting the Putative GRPE Element and the Region Separating GRPE and Ψ on Packaging of the 5′LTR sgRNA

(A) The putative GRPE was deleted as a 1,819–2,251 and 1,956–2,188 nt region in the p1–p6 coding regions of *gag* within the pREC-5′LTR-RT$_{2845}$, which was then cotransfected with pREC-nfl-3′LTR in 293T cells. A similar GRPE region was also deleted from the WT pNL4-3 construct and cotransfected with the pCMVΔR8.91 vector (D). Finally, four regions were deleted separating the putative GRPE from Ψ (E). The gRNAs were quantified in virus particles by qRT-PCR as described in Figure 3 and presented as copies/ul in (B), (D), and (F) for the 5′LTR sgRNAs (or NL4-3 gRNA) and for the nfl-3′LTR sgRNA in Figure S4. Virus infectivity was

(legend continued on next page)

Quantitation of the sgRNAs in virus particles revealed that the 868 nt deletion within the *gag* coding sequence of 5′LTR sgRNA (Figure 4E) had WT gRNA packaging levels. However, the 5′LTR-MA$_{1208}$ sgRNA, analogous to removal of the GRPE from 5′LTR-p6Δ868 sgRNA, resulted in a 59-fold decrease in sgRNA packaging (Figure 4F). Secondary structure analyses of 5′LTR-p6Δ868 sgRNA using SHAPE/RNAstructure (Mathews et al., 2004) revealed that the structure of the RFS/GRPE (Figure 4H) closely resembles the SHAPE-derived RNA structure obtained using gRNA isolated from HIV-1 particles (Watts et al., 2009). This structure is characteristic of a type C three-way junction (Lescoute and Westhof, 2006) connecting a stem and two stem loops (P2 and P3). P2SL contains the "slippery sequence" flanked at the 3′ end by the continuous, P3SL, which is essential for Gag-Pol ribosomal frameshifting (Dulude et al., 2002).

Surprisingly, deleting a smaller region in 5′LTR-p6Δ706 and 5′LTR-p6Δ716 sgRNA (Figure 4E) severely reduced sgRNA packaging (Figure 4F) despite retaining the entire linear GRPE sequence found in 5′LTR-p6Δ868 sgRNA (with WT packaging efficiency). In these cases, the 3′ ends of the RNA in 5′LTR-p6Δ707 and 5′LTR-p6Δ716 sgRNA were truncated to nucleotides 2,270 and 2,183 (Figure 4E), respectively. Probing of these two protein-free sgRNAs showed substantial destabilization of P2SL (Figure 4H). Specifically, the 5′LTR-p6Δ707 and 5′LTR-p6Δ716 sgRNA showed high 1M7 reactivity within residues forming P2SL. Moreover, nucleotides 2,044–2,049 show enhanced reactivity compared to 5′LTR-p6Δ868 sgRNA, suggesting they no longer base pair with the segment spanning nucleotides 2,132–2,137 (Figure 4H). In contrast, nucleotides 2,096–2,098, reactive in the 5′LTR-p6Δ868 sgRNA, were unreactive in these sgRNAs and are instead predicted to be involved in forming an extended, discontinuous P3 hairpin (Figure 4H). These data suggest that although the GRPE may function independent of sequence context, both the P2 and P3SL must be maintained for enhanced packaging activity. This observation was confirmed by deleting 996 nt of the *gag* sequence (Δ1091–2085) in 5′LTR-p6Δ996 sgRNA to remove the linear sequence encoding P2SL, which dramatically reduced packaging (Figure 4F). Again, the nfl-3′LTR sgRNAs were encapsidated at a stable level (Figure S4B). Reduced packaging of the 5′LTR sgRNA with these internal deletions resulted in decreased infectivity of U87.CD4.CXCR4 cells (Figure 4G). In the case of the 5′LTR-p6Δ868 sgRNA, increased infectivity (10^3 IU/ml) was less than expected considering the high level of 5′LTR-p6Δ868 sgRNA packaging (Figure 4F). As discussed later, intervening RNA sequences (also hidden in the coding sequence) may impact other sgRNA functions aside from encapsidation, such as dimerization, tRNA^{Lys,3} placement, or initiation of reverse transcription.

Effect of GRPE Secondary Structure on gRNA Encapsidation, Dimerization, and Virus Infectivity

To further probe the impact of the P2 and P3 stem loops in RNA packaging, we preformed site-directed mutagenesis based on

M-fold RNA structure predictions. Mutations (Figure 5A) causing minor rearrangement in the general structure of both P2 and P3SL (mu1, mu2, and mu4 in Figure 5B) had minimal effects on 5′LTR sgRNA encapsidation (1.1-, 2.2-, and 3.2-fold, respectively) (Figure 5C) and only slight losses in infectivity (Figure 5E). In contrast, when M-fold predicted significant changes to P2 and P3SL with the 4 nt and 3 nt substitutions in mu3 and mu5 sgRNAs (Figures 5A and 5B), a 13.5- and 28-fold reduction was observed in packaging which corresponded to a 560- and 1,400-fold loss of infectivity, respectively (Figures 5C and 5E). Similar to previous experiments, the levels of nfl-3′LTR sgRNA packaging remained constant with all the mu 5′LTR sgRNAs (Figure 5D). These studies provided the strongest evidence for the importance of the P2 and P3SL for sgRNA packaging.

Exploring the Relationship between HIV-1 mRNA Translation and gRNA Packaging

The GRPE overlaps with the sequences and/or structures involved in ribosomal frameshifting, but linking factors involved in translation with processes involved in gRNA packaging will require more detailed studies. The translation termination factor eRF1 binds to the termination codon, stops translation via interactions with the ribosome, and helps to initiate the nonsense RNA decay (NMD) pathway (Nicholson et al., 2010). Previous studies indicate that siRNA knockdown of eRF1 increased Gag-Pol synthesis relative to Gag, suggesting increased ribosomal frameshifting and loss of infectivity (Kobayashi et al., 2010).

To explore the possible role of eRF1 and ribosomal frameshifting on gRNA packaging, we downregulated cellular levels of eRF1 with siRNA (Figure 6A), but failed to observe an increase in Gag-Pol in virus particles (data not shown). Next, we measured levels of 5′LTR sgRNAs (by qRT-PCR) relative to RT activity (or relative to p24 content of the virus). When eRF1 was depleted with siRNA knockdown, the amount of 5′LTR sgRNA increased >10-fold as compared to virus produced in the presence of scrambled siRNA (Figure 6B). Based on the assumption of ~2,000 Gag dimers per WT virus particles, knockdown of eRF1 appears to have produced virus particles containing ~15–20 genomic RNAs. We performed the same eRF1 knockdown experiment with an HIV molecular clone (NL4-3 based) that carries a Gag-interdomain green fluorescent protein (iGFP) (Hübner et al., 2007). HIV Gag-iGFP was transfected into 293T cells to produce virus harboring a Gag-GFP fusion. Reductions in eRF1 (Figure 6C) appear to result in virus particles with more gRNA per Gag molecule (Figure 6D) as well as brighter fluorescence (compare Figures 6E and 6F), suggesting enlarged virus particles containing more of Gag, Gag-Pol, and gRNA.

gRNA Dimerization, GRPE, and Model of gRNA Packaging

The following discussion and Figure 7 highlight how ribosomal frameshifting and gRNA packaging may be tightly regulated. Dimerization is described as being an early event during gRNA

---

measured by first normalizing for RT activity, serially diluting as described in Figure 2C, and then adding to U87.CD4.CXCR4 cells (Figure 2D). The level of infectious virus is presented as log$_{10}$ infectious units/ml in (C) and (G). The structure of the sgRNA was analyzed using SHAPE (Watts et al., 2009) and presented in (H) using the modeling algorithm RNAstructure (Mathews et al., 2004). Full-length in vitro-transcribed 5′LTR sgRNA (E) was used for structural probing, but only the region proximal to GRPE/RFS was presented in (H). Data in (B), (D), and (F) are presented as mean ± SEM. See also Figure S4.
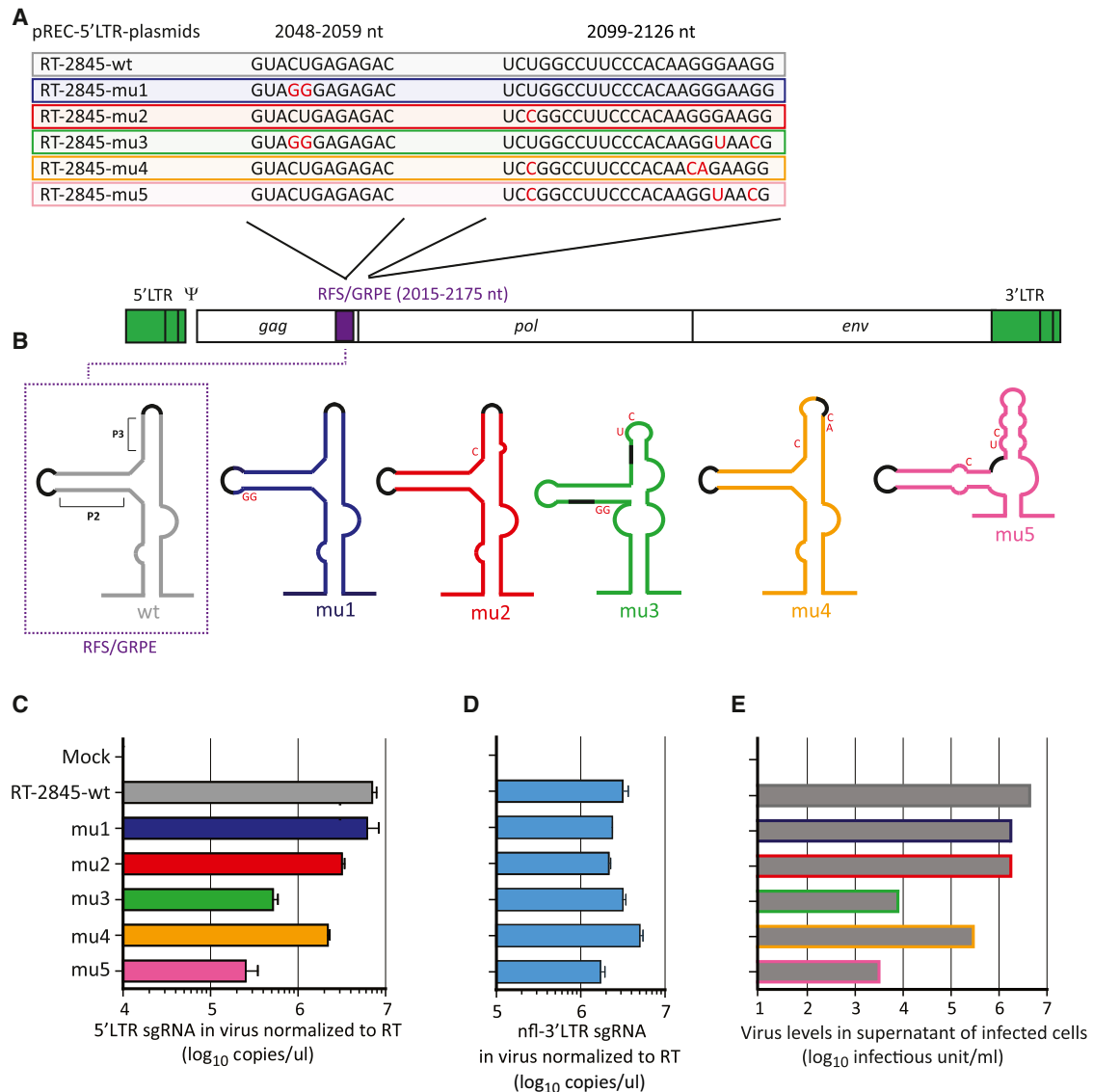
Figure 5. The Role of RNA Secondary Structure in the GRPE/RFS Region on HIV-1 RNA Packaging
(A) Multiple point mutations were introduced to the predicted P2 and P3 stem loops within the GRPE/RFS sequence. (B) The RNA secondary structures in the GRPE/RFS region of these five mutants were predicted by M-fold (http://mfold.rna.albany.edu/). The five mutant 5′LTR sgRNA templates were expressed in cotransfected 293T cells. Supernatants from these transfected cells were harvested to measure 5′LTR sgRNA (C) and nfl-3′LTR sgRNA levels (D) by q-RT-PCR. The same virus-containing supernatant was then equalized for RT activity, serially diluted, and used to infect U87.CD4.CXCR4 cells. The relative infectivity, as measured by $TCID_{50}$ assay, is presented as log_{10} infectious units/ml (E). Data in (C) and (D) are presented as mean ± SEM.

capture/transport and linked to the 5′UTR (Paillart et al., 2004; Johnson and Telesnitsky, 2010; Clever and Parslow, 1997; Skripkin et al., 1994). To determine the impact of GRPE on gRNA dimerization, we performed in vitro RNA dimerization experiments using 3′LTR and 5′LTR RNAs ± GRPE (all containing the DIS) (Figure S5). We observed efficient in vitro dimerization of all sgRNAs (either 5′LTR- or 3′LTR-containing RNAs) regardless of the presence or absence of the GRPE (Figures S5A and S5C). In fact, the shortest 5′LTR RNA (MA-1208) dimerizes with high efficiency (>70% in loose dimers) but cannot be packaged efficiently (>51-fold decrease). Oligonucleotides annealing to DIS could disrupt dimer formation (Figure S5B). These in vitro find-

ings may or may not reflect HIV-1 gRNA dimerization in the cell during encapsidation, but our model in Figure 7 now suggests that GRPE is involved in gRNA encapsidation following loose dimer formation.

DISCUSSION

Studies starting in the late 1970s discovered that avian and murine retroviruses preferentially packaged full-length viral RNA over the pool of cellular RNAs or spliced viral mRNA (Gerwin and Levin, 1977). Groundbreaking papers by Shank and Linial (Linial et al., 1978; Shank and Linial, 1980) first described
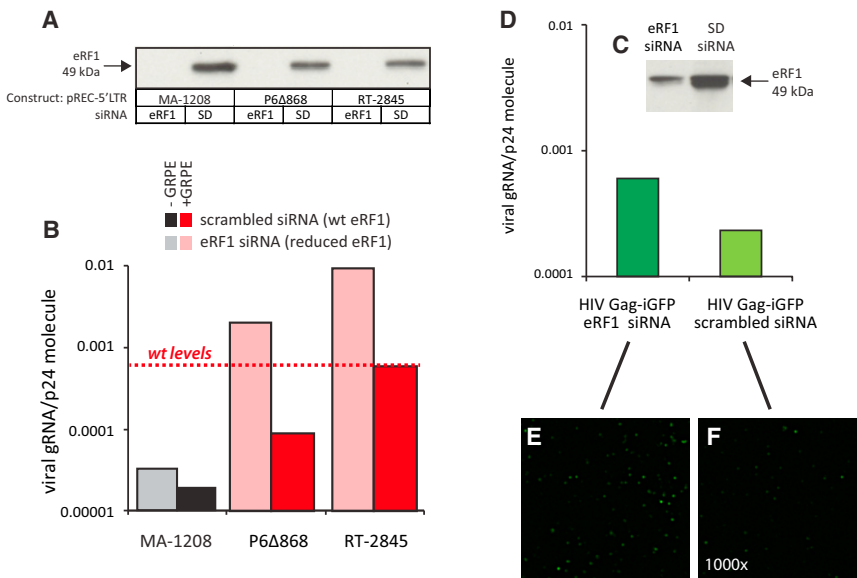
Figure 6. The Effect of eRF1 Knockdown on Virus Production and gRNA Encapsidation

A pool of three siRNAs against eRF1 effectively reduces cellular eRF1 expresion level by ~70% prior to 293T transfections as indicated by western blot analysis (A) and (C) These siRNA-treated 293T cells were cotransfected with the pREC-nfl-3′LTR along with either pREC-5′LTR-MA$_{1208}$, pREC-5′LTR-p6Δ868, or pREC-5′LTR-RT$_{2845}$ or transfected with HIV Gag-iGFP. It is important to note that eRF1 knockdown reduced all protein levels in the cell 2-fold within 72 hr. Virus produced from these siRNA-treated, cotransfected cells was noninfectious for U87.CD4.CXCR4 cells. The 5′LTR sgRNA or NL4-3 gRNA in virus particles was measured by qRT-PCR and presented as relative to p24 antigen content (B) and (D). In the presence of WT levels of eRF1 (SD siRNA treatment), the virus produced from the cotransfected cells harbored approximately 1.6 5′LTR sgRNA copies per 2,000 molecules of p24 (or the estimated size of one HIV-1 particle). With the eRF1 knockdown and the WT pREC-5′LTR-RT$_{2845}$, there are approximately 19 5′LTR sgRNA copies per 2,000 p24 molecules. Virus derived from transfections with the HIV Gag-iGFP molecular clone (E, eRF1 knockdown; F, WT eRF1) was sucrose-cushion purified, spread on poly-L-lysine coverslips, and images captured on a Deltavision RT epifluorescent microscope system.

a 300 bp region upstream of the *gag-pol* genes in avian sarcoma virus (ASV) necessary for preferential packaging of the ASV RNA genome, and this Ψ still remains the quintessential packaging element for almost all retroviruses including HIV-1 (Lever et al., 1989).

By dividing the genome into two sgRNAs (5′LTR-nfl and nfl-3′LTR sgRNA), we established a system in which only heterodiploid virus can establish de novo infection following completion of reverse transcription. In the infected cells, the 5′LTR-nfl sgRNA binds with tRNA^{Lys,3} and serves as a template for (−) strong stop DNA but does not contribute to the HIV-1 coding sequence within the integrated genome. We performed a series of RNA truncations, deletions, and point mutations within 5′LTR-nfl sgRNA to identify and characterize a previously unrecognized RNA packaging element at the 3′ end of *gag*. Removing the GRPE from 5′LTR-nfl sgRNA did not impact virus production from transfected cells but resulted in a >50-fold loss in packaging of 5′LTR-nfl sgRNA relative to nfl-3′LTR sgRNA, paralleled by the loss in virus infectivity. Even with this two log decrease, residual virus infectivity levels suggest that the Ψ/5′UTR is required for low levels of gRNA packaging.

In our system, the nfl-3′LTR sgRNA lacks TAR hairpin and poly(A) loops, shown to have modest effects on gRNA encapsidation (Russell et al., 2003; McBride and Panganiban, 1996; Clavel and Orenstein, 1990; Rizvi et al., 2010). Vrolijk et al. propose that these elements (located upstream of SD) must work in coordination with the major packaging signal, found only in the unspliced HIV-1 RNA (Vrolijk et al., 2008). We examined the GRPE effect in the context of a full-length HIV-1 genome (with both LTRs intact) and found that the deletion of GRPE still reduced gRNA packaging (Figure 4D). The GPRE deletion with the bipartite genome system resulted in 14-fold reduction in gRNA packaging, whereas a 7-fold decrease was observed with the deletion of GRPE in WT NL4-3. The slightly reduced

effect of the GRPE with an intact 5′LTR suggests a modest impact of the TAR on gRNA packaging: ~2-fold as reported (Clavel and Orenstein, 1990; McBride and Panganiban, 1996; Russell et al., 2003). Finally, we discovered that the GRPE is absent in most single-cycle lentiviral systems used for gene therapy, biochemical studies, or vaccine development. Preliminary studies suggest that introducing the GRPE within a lentiviral gene delivery vector, even out of sequence context, can result in a >10-fold increase in transduction and gene delivery, which is directly related to increased gRNA encapsidation (M.C. and E.J.A., unpublished data).

The RNA packaging element is often described as a set of static, discrete RNA hairpin structures. However, structural studies involving combination of bioinformatics, enzymatic probing, and phylogenetic and intramolecular UV-crosslinking techniques suggest structural transitions involving both local multiple branched hairpins near Ψ as well as some long-distance interactions at the 5′ end of gRNA (Damgaard et al., 2004; Abbink and Berkhout, 2003; Huthoff and Berkhout, 2001). Furthermore, a riboswitch might help to regulate gRNA dimerization and packaging. NMR studies revealed a long-distance interaction whereby the DIS interacts with U5 to inhibit the dimerization, while an alternative conformation releases the AUG start codon to promote the translation (Lu et al., 2011). We are currently exploring how the GRPE may factor into this regulation and promote gRNA packaging. Our preliminary in vitro studies suggest that the GRPE does not impact RNA dimerization of either the 5′LTR or 3′LTR sqRNAs, whereas disruption of the DIS did prevent dimerization as previously described (Skripkin et al., 1994). Although loose RNA dimer formation may have some relation to the in vivo event, there are obviously cellular and viral factors that are absent in vitro (e.g., NC region of Gag) that are required for maturation of tight dimers and encapsidation (Paillart et al., 2004; Johnson and Telesnitsky, 2010).
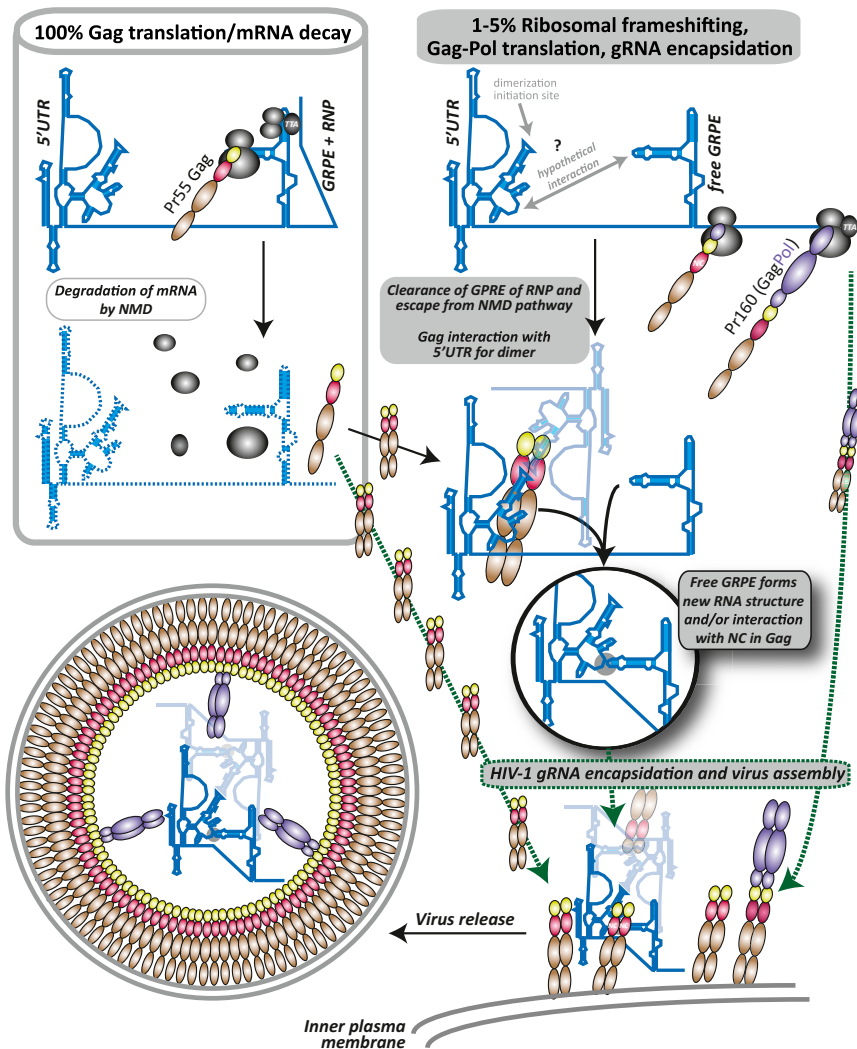
Figure 7. Model for Translation and Packaging of the Unspliced HIV-1 RNA
Unspliced mRNA is destined for (1) Gag translation and subsequent substrate for NMD pathway or (2) may serve as a template Gag-Pol translation following ribosomal frameshift and thus avoiding NMD (<5%). Ribosomal translocation across the unspliced mRNA used for Gag-Pol translation may clear the RNA of cellular factors (e.g., eRF1) and thus promote secondary/tertiary HIV-1 RNA, resulting in RNA-protein interactions necessary for gRNA dimerization following by packaging. MA, matrix; CA, capsid; NC, nucleocapsid. See also Figure S5.

also suspect higher-order structures between Ψ and GRPE, but at this stage a series of detailed biochemical studies involving SHAPE and/or high resolution NMR are necessary to support these claims. Nonetheless, biochemical studies presented herein provide evidence for intricate transition events designating an HIV-1 unspliced RNA as (1) an mRNA for Gag translation or (2) an mRNA for Gag-Pol translation and gRNA for encapsidation.

Overlap between the GRPE and the RFS suggested a possible link between translation and gRNA packaging. In relation to translation termination, eRF1 mediates peptidyl-tRNA hydrolysis at the peptidyl transferase center of the ribosome to terminate translation. eRF1 also nucleates a host protein complex involved in 3′UTR sensing and the NMD pathway (Hogg and Goff, 2010). In 2010, Kobayashi et al. identified eRF1 from

As described herein, we show that the GRPE cannot act alone for gRNA packaging but likely involves the Ψ and related 5′UTR sequences.

The importance of the two GRPE stem loops for gRNA packaging was evident with point mutations and deletions of intervening sequences between the GRPE and 5′UTR. Efficient gRNA packaging was maintained with point mutations or deletions that had minor effects on the stability of P2 and P3SL as revealed by SHAPE analyses. Aside from their role in gRNA packaging as described here, these two stem loops are also necessary for ribosomal frameshifting, a mechanism conserved among all lentiviruses. Most retroviruses employ a readthrough translation mechanism whereby a transient/infrequent RNA pseudoknot may stall the ribosome at the UAG stop codon, leading to a glutamine incorporation (Houck-Loomis et al., 2011). Although there is no experimental evidence for involvement of RNA pseudoknots in lentiviral frameshifting, in vitro SHAPE analyses on the static GRPE sequence provide some support for possible pseudoknot involving the P2 and P3SL, but this would also infer a complete unwinding of these two SLs (M.C., K.J.P., S.F.J.L., and E.J.A., unpublished data). We

a genome-wide siRNA knockdown screen as a putative candidate for interactions with ribosomal frameshift site (Kobayashi et al., 2010). In their studies, eRF1 depletion led to increased ratio of Gag-Pol:Gag in HIV-infected cells and production of noninfectious virus. As a preliminary study, we reduced eRF1 expression levels with siRNAs in cells subsequently transfected with our WT and GRPE mutant HIV-1 constructs. Reducing eRF1 levels increased encapsidation of HIV-1 gRNA relative to CA p24 levels in the cell-free supernatant. These virus-like particles may contain >20 times more gRNA than wild-type virus based on an assumption of 2,000 Gag dimers per virus particle. When using a virus containing Gag-iGFP, knockdown of eRF1 appears to mediate production of "large" virus particles with more Gag (brighter virus particles) and more gRNA. Based on these preliminary results and positioning of the GRPE, we propose that Gag-Pol ribosomal frameshifting may prevent the NMD pathway and designate this unspliced HIV-1 mRNA (destined for translation of Gag-Pol) as gRNA for encapsidation. Thus, even slight increases in ribosomal frameshifting and Gag-Pol synthesis could lead to dramatic increases in gRNA levels and release of noninfectious virus particles. Figure 7 presents a model on the

control of HIV-1 translation, ribosomal frameshifting, and gRNA packaging by the GRPE/RFS. A complex involving eRF1 may form at or near the GRPE/RFS during translation. Termination of translation may initiate mRNA degradation by the NMD pathway via accumulation of Up-frameshift protein 1 (Upf1) on the extended 3′UTR and thus prevent Gag precursor binding to this RNA for encapsidation (Hogg and Goff, 2010). In <5% of translation events on unspliced HIV-1 mRNA, the ribosome may shift −1 nt at the RFS, clear the GRPE, prevent binding Upf1-dependent decay complex, and promote interactions of cytoplasmic poly(A)-binding protein 1 (PABPC1) with eRF1/eRF3 (Ivanov et al., 2008) to eventually terminate Gag-Pol translation. This rare event in HIV-1 translation would maintain a stable unspliced HIV-1 RNA where the GRPE may be free to participate in higher-order RNA interactions (possibly with Ψ) and/or interact with HIV-1 Gag (or additional cellular factors). Thus, the unspliced mRNA which was used as a template for Gag-Pol translation would also serve as genomic RNA. This model also supports the notion that only a few Gag precursor proteins can bind HIV-1 unspliced mRNA for encapsidation prior to virus assembly leaving the majority of Gag precursors to form the virus core during assembly. Again, this process of virus assembly and correct gRNA encapsidation would be tightly regulated by GRPE, a highly conserved HIV-1 sequence.

EXPERIMENTAL PROCEDURES

Additional details of the experimental procedures are provided in the Supplemental Experimental Procedures.

Plasmids

All plasmids in this study were initially prepared using yeast-based recombination/gap repair system as described (Dudley et al., 2009). Details of base pREC-5′LTR and pREC-nfl-3′LTR vectors and cloning are provided in the Supplemental Experimental Procedures.

Transfection and Infection

293T cells were cotransfected with pREC-5′LTR and pREC-nfl-3′LTR plasmids (~3 μg of each plasmid) using FuGENE6 (Roche). Cells and cell-free supernatant were harvested 48 hr posttransfection to measure infectious titers by RT assay (Gao et al., 2009) and viral protein levels by western blot and p24 antigen capture assays (see the Supplemental Experimental Procedures for details). Cellular and viral RNAs were extracted using the RNeasy kit (QIAGEN) and MagMax (Ambion) kits, respectively, to determine levels of HIV-1 RNA expression and encapsidation. Cytoplasmic and nuclear RNA isolations were performed using the PARIS Kit (Ambion). Correct fractionation of cytoplasmic and nuclear RNA was tested by RT-PCR amplifying the spliced and unspliced actin (respectively) with the OTR580, OTR581, and OTR582 primers.

Quantitative Real-Time PCR

Cell- and virion-associated RNAs were reverse transcribed using specific primer Gag 820–796 for 5′LTR-cDNA and oligo dt primer (Invitrogen) for nfl-3′LTR c-DNA using Superscript III transcriptase (Invitrogen). The ABI PRISM 7000 sequence detection system (Applied Biosystems) was used for qRT-PCR amplifications. U5 and U3 target sequences were specifically amplified using primer pairs and probes described in Figure 3A. 18S ribosomal RNA was amplified as an internal control for cellular RNA with the forward primer human R18.seq-948F and reverse primer human R18.seq-1014R, and detected with probe 6FAM-TAMRA-3′ (Table S1). Serial dilutions of plasmid DNA with known copy numbers provided amplification and quantitation controls. For 18 s ribosomal RNA standard, Quantuserial dilution of mRNA Universal 18S Internal Standard (Ambion) was used. Lack of plasmid DNA contamination from transfection of cells was confirmed by a control excluding reverse transcriptase (RT).

RNA Synthesis and Secondary RNA Structure Prediction Analysis

Briefly, in vitro-transcribed RNAs were purified using MEGAclear kit (Ambion), and the size and integrity were checked by denaturing formaldehyde agarose gel electrophoresis. Fluorescently labeled primer (1 μl) was annealed to 2.5 pmols of RNA (Cy5 [+] and Cy5.5 [−]; 8 μM), then reverse transcribed. Primer extension products were analyzed using a Beckman CEQ8000 Genetic Analysis System. Electropherograms were processed using the ShapeFinder software. 1M7 reactivity at each nucleotide position was normalized as described (Wilkinson et al., 2008). Resulting data were introduced to the RNAstructure software as pseudoenergy constraints. Secondary structures were visualized using PseudoViewer web application (http://pseudoviewer.inha.ac.kr/). M-fold web server (http://mfold.rna.albany.edu/) was used to predict secondary structures of RNA mutants.

SUPPLEMENTAL INFORMATION

Supplemental Information includes five figures, two tables, Supplemental Experimental Procedures, and Supplemental References and can be found with this article at http://dx.doi.org/10.1016/j.chom.2013.01.007.

REFERENCES

Abbink, T.E., and Berkhout, B. (2003). A novel long distance base-pairing interaction in human immunodeficiency virus type 1 RNA occludes the Gag start codon. J. Biol. Chem. 278, 11601–11611.

Aldovini, A., and Young, R.A. (1990). Mutations of RNA and protein sequences involved in human immunodeficiency virus type 1 packaging result in production of noninfectious virus. J. Virol. 64, 1920–1926.

Amarasinghe, G.K., De Guzman, R.N., Turner, R.B., Chancellor, K.J., Wu, Z.R., and Summers, M.F. (2000). NMR structure of the HIV-1 nucleocapsid protein bound to stem-loop SL2 of the psi-RNA packaging signal. Implications for genome recognition. J. Mol. Biol. 301, 491–511.

Berkowitz, R., Fisher, J., and Goff, S.P. (1996). RNA packaging. Curr. Top. Microbiol. Immunol. 214, 177–218.

Burniston, M.T., Cimarelli, A., Colgan, J., Curtis, S.P., and Luban, J. (1999). Human immunodeficiency virus type 1 Gag polyprotein multimerization requires the nucleocapsid domain and RNA and is promoted by the capsid-dimer interface and the basic region of matrix protein. J. Virol. 73, 8527–8540.

Clavel, F., and Orenstein, J.M. (1990). A mutant of human immunodeficiency virus with reduced RNA packaging and abnormal particle morphology. J. Virol. 64, 5230–5234.

Clever, J.L., and Parslow, T.G. (1997). Mutant human immunodeficiency virus type 1 genomes with defects in RNA dimerization or encapsidation. J. Virol. 71, 3407–3414.

Damgaard, C.K., Andersen, E.S., Knudsen, B., Gorodkin, J., and Kjems, J. (2004). RNA interactions in the 5′ region of the HIV-1 genome. J. Mol. Biol. 336, 369–379.

Davis, N.L., and Rueckert, R.R. (1972). Properties of a ribonucleoprotein particle isolated from Nonidet P-40-treated Rous sarcoma virus. J. Virol. 10, 1010–1020.

De Guzman, R.N., Wu, Z.R., Stalling, C.C., Pappalardo, L., Borer, P.N., and Summers, M.F. (1998). Structure of the HIV-1 nucleocapsid protein bound to the SL3 psi-RNA recognition element. Science 279, 384–388.

D'Souza, V., and Summers, M.F. (2005). How retroviruses select their genomes. Nat. Rev. Microbiol. *3*, 643–655.

Dudley, D.M., Gao, Y., Nelson, K.N., Henry, K.R., Nankya, I., Gibson, R.M., and Arts, E.J. (2009). A novel yeast-based recombination method to clone and propagate diverse HIV-1 isolates. Biotechniques *46*, 458–467.

Dulude, D., Baril, M., and Brakier-Gingras, L. (2002). Characterization of the frameshift stimulatory signal controlling a programmed −1 ribosomal frameshift in the human immunodeficiency virus type 1. Nucleic Acids Res. *30*, 5094–5102.

Gao, Y., Nankya, I., Abraha, A., Troyer, R.M., Nelson, K.N., Rubio, A., and Arts, E.J. (2009). Calculating HIV-1 infectious titre using a virtual TCID(50) method. Methods Mol. Biol. *485*, 27–35.

Gerwin, B.I., and Levin, J.G. (1977). Interactions of murine leukemia virus core components: characterization of reverse transcriptase packaged in the absence of 70S genomic RNA. J. Virol. *24*, 478–488.

Hogg, J.R., and Goff, S.P. (2010). Upf1 senses 3′UTR length to potentiate mRNA decay. Cell *143*, 379–389.

Houck-Loomis, B., Durney, M.A., Salguero, C., Shankar, N., Nagle, J.M., Goff, S.P., and D'Souza, V.M. (2011). An equilibrium-dependent retroviral mRNA switch regulates translational recoding. Nature *480*, 561–564.

Hu, W.S., and Temin, H.M. (1990). Retroviral recombination and reverse transcription. Science *250*, 1227–1233.

Hübner, W., Chen, P., Del Portillo, A., Liu, Y., Gordon, R.E., and Chen, B.K. (2007). Sequence of human immunodeficiency virus type 1 (HIV-1) Gag localization and oligomerization monitored with live confocal imaging of a replication-competent, fluorescently tagged HIV-1. J. Virol. *81*, 12596–12607.

Huthoff, H., and Berkhout, B. (2001). Two alternating structures of the HIV-1 leader RNA. RNA *7*, 143–157.

Ivanov, P.V., Gehring, N.H., Kunz, J.B., Hentze, M.W., and Kulozik, A.E. (2008). Interactions between UPF1, eRFs, PABP and the exon junction complex suggest an integrated model for mammalian NMD pathways. EMBO J. *27*, 736–747.

Jacks, T., Power, M.D., Masiarz, F.R., Luciw, P.A., Barr, P.J., and Varmus, H.E. (1988). Characterization of ribosomal frameshifting in HIV-1 gag-pol expression. Nature *331*, 280–283.

Johnson, S.F., and Telesnitsky, A. (2010). Retroviral RNA dimerization and packaging: the what, how, when, where, and why. PLoS Pathog. *6*, e1001007. http://dx.doi.org/10.1371/journal.ppat.1001007.

Kobayashi, Y., Zhuang, J., Peltz, S., and Dougherty, J. (2010). Identification of a cellular factor that modulates HIV-1 programmed ribosomal frameshifting. J. Biol. Chem. *285*, 19776–19784.

Kutluay, S.B., and Bieniasz, P.D. (2010). Analysis of the initiating events in HIV-1 particle assembly and genome packaging. PLoS Pathog. *6*, e1001200. http://dx.doi.org/10.1371/journal.ppat.1001200.

Lescoute, A., and Westhof, E. (2006). Topology of three-way junctions in folded RNAs. RNA *12*, 83–93.

Lever, A., Gottlinger, H., Haseltine, W., and Sodroski, J. (1989). Identification of a sequence required for efficient packaging of human immunodeficiency virus type 1 RNA into virions. J. Virol. *63*, 4085–4087.

Linial, M., Medeiros, E., and Hayward, W.S. (1978). An avian oncovirus mutant (SE 21Q1b) deficient in genomic RNA: biological and biochemical characterization. Cell *15*, 1371–1381.

Lu, K., Heng, X., Garyu, L., Monti, S., Garcia, E.L., Kharytonchyk, S., Dorjsuren, B., Kulandaivel, G., Jones, S., Hiremath, A., et al. (2011). NMR detection of structures in the HIV-1 5′-leader RNA that regulate genome packaging. Science *334*, 242–245.

Marozsan, A.J., Fraundorf, E., Abraha, A., Baird, H., Moore, D., Troyer, R., Nankja, I., and Arts, E.J. (2004). Relationships between infectious titer, capsid protein levels, and reverse transcriptase activities of diverse human immunodeficiency virus type 1 isolates. J. Virol. *78*, 11130–11141.

Mathews, D.H., Disney, M.D., Childs, J.L., Schroeder, S.J., Zuker, M., and Turner, D.H. (2004). Incorporating chemical modification constraints into a dynamic programming algorithm for prediction of RNA secondary structure. Proc. Natl. Acad. Sci. USA *101*, 7287–7292.

McBride, M.S., and Panganiban, A.T. (1996). The human immunodeficiency virus type 1 encapsidation site is a multipartite RNA element composed of functional hairpin structures. J. Virol. *70*, 2963–2973.

Nicholson, P., Yepiskoposyan, H., Metze, S., Zamudio Orozco, R., Kleinschmidt, N., and Mühlemann, O. (2010). Nonsense-mediated mRNA decay in human cells: mechanistic insights, functions beyond quality control and the double-life of NMD factors. Cell. Mol. Life Sci. *67*, 677–700.

Paillart, J.C., Shehu-Xhilaga, M., Marquet, R., and Mak, J. (2004). Dimerization of retroviral RNA genomes: an inseparable pair. Nat. Rev. Microbiol. *2*, 461–472.

Rein, A. (1994). Retroviral RNA packaging: a review. Arch. Virol. Suppl. *9*, 513–522.

Rizvi, T.A., Kenyon, J.C., Ali, J., Aktar, S.J., Phillip, P.S., Ghazawi, A., Mustafa, F., and Lever, A.M. (2010). Optimal packaging of FIV genomic RNA depends upon a conserved long-range interaction and a palindromic sequence within gag. J. Mol. Biol. *403*, 103–119.

Russell, R.S., Hu, J., Bériault, V., Mouland, A.J., Laughrea, M., Kleiman, L., Wainberg, M.A., and Liang, C. (2003). Sequences downstream of the 5′ splice donor site are required for both packaging and dimerization of human immunodeficiency virus type 1 RNA. J. Virol. *77*, 84–96.

Shank, P.R., and Linial, M. (1980). Avian oncovirus mutant (SE21Q1b) deficient in genomic RNA: characterization of a deletion in the provirus. J. Virol. *36*, 450–456.

Skripkin, E., Paillart, J.C., Marquet, R., Ehresmann, B., and Ehresmann, C. (1994). Identification of the primary site of the human immunodeficiency virus type 1 RNA dimerization in vitro. Proc. Natl. Acad. Sci. USA *91*, 4945–4949.

Swanson, C.M., and Malim, M.H. (2006). Retrovirus RNA trafficking: from chromatin to invasive genomes. Traffic *7*, 1440–1450.

Vrolijk, M.M., Ooms, M., Harwig, A., Das, A.T., and Berkhout, B. (2008). Destabilization of the TAR hairpin affects the structure and function of the HIV-1 leader RNA. Nucleic Acids Res. *36*, 4352–4363.

Watts, J.M., Dang, K.K., Gorelick, R.J., Leonard, C.W., Bess, J.W., Jr., Swanstrom, R., Burch, C.L., and Weeks, K.M. (2009). Architecture and secondary structure of an entire HIV-1 RNA genome. Nature *460*, 711–716.

Wilkinson, K.A., Gorelick, R.J., Vasa, S.M., Guex, N., Rein, A., Mathews, D.H., Giddings, M.C., and Weeks, K.M. (2008). High-throughput SHAPE analysis reveals structures in HIV-1 genomic RNA strongly conserved across distinct biological states. PLoS Biol. *6*, e96. http://dx.doi.org/10.1371/journal.pbio.0060096.

Wilson, W., Braddock, M., Adams, S.E., Rathjen, P.D., Kingsman, S.M., and Kingsman, A.J. (1988). HIV expression strategies: ribosomal frameshifting is directed by a short sequence in both mammalian and yeast systems. Cell *55*, 1159–1169.